Interactions among Residues CD3, E7, E10, and E11 in Myoglobins: Attempts To Simulate the Ligand-Binding Properties of *Aplysia* Myoglobin[†,‡]

Stephen J. Smerdon, Szymon Krzywda, Andrzej M. Brzozowski, Gideon J. Davies, and Anthony J. Wilkinson*

Department of Chemistry, University of York, York YO1 5DD, U.K.

Andrea Brancaccio, Francesca Cutruzzolá, Carlo Travaglini Allocatelli, and Maurizio Brunori

Department of Biochemical Sciences, "A. Rossi Fanelli" and CNR Centre for Molecular Biology, University of Rome "La Sapienza", 00185 Rome, Italy

Tiansheng Li, Robert E. Brantley, Jr., Theodore E. Carver, Raymund F. Eich, Eileen Singleton, and John S. Olson

Department of Biochemistry and Cell Biology and W. M. Keck Center for Computational Biology, Rice University, Houston, Texas 77005-1892

Received January 23, 1995; Revised Manuscript Received April 20, 1995[⊗]

ABSTRACT: Site-directed mutations have been introduced singly and in combination at residues lysine/arginine[45] (CD3), histidine[64] (E7), threonine[67] (E10), and valine[68] (E11) in pig and sperm whale myoglobins. The mutations probe the roles of these key distal pocket residues and represent attempts to mimic the heme environment of *Aplysia limacina* myoglobin which achieves moderately high O_2 affinity in the absence of a distal histidine. In the mollusc myoglobin, arginine-E10 is believed to swing into the heme pocket and provide a hydrogen bond to the bound O_2. The association and dissociation rate constants for oxygen and carbon monoxide binding to H64V, T67A, T67V, T67E, T67R, V68I, V68T, H64V-T67R, H64V-V68T, H64V-V68I, and H64V-T67R-V68I pig myoglobin mutants and T67R, H64V-T67R, and R45D-H64V-T67R mutants of sperm whale myoglobin have been measured using stopped-flow rapid mixing and flash photolysis techniques. Replacement of histidine-E7 with valine in either pig or sperm whale myoglobin drastically lowers O_2 affinity while increasing CO affinity. Two second-site mutations, T67R and V68T, increase O_2 affinity in the H64V mutant, even though when introduced singly these mutations have no effect or lower K_{O_2}, respectively. However, the oxygen affinities of the H64V-T67R mutants are 5−10-fold lower than that of *A. limacina* myoglobin. The crystal structure of the pig H64V-T67R double mutant reveals that the valine-E7 side chain is ~1 Å closer to the heme plane than in the mollusc protein which may restrict access of the arginine-E10 side chain into the heme pocket. The O_2 affinity of the H64V-T67R double mutant is not altered by the R45D replacement but is reduced 10-fold by the V68I mutation. The interactive effects of the T67R, V68I, and V68T mutations with the H64V substitution are discussed in terms of O_2, CO, and N_3^- binding and the crystal structures of the H64V-T67R, H64V-V68I, and H64V-V68T double-mutant proteins. In many instances, the effects of second-site mutations in the valine[64] background are the opposite of those observed for the corresponding single mutations in the wild type background. These results can be understood in terms of the changes in the rate-determining steps for ligand association and dissociation and the loss of distal pocket water molecules which follow replacement of histidine[64] by valine.

The reversible binding of dioxygen by myoglobin and hemoglobin is central to the metabolism of vertebrates and invertebrates, providing a reservoir of O_2 that is available for aerobic respiration. Hydrogen bonding between the distal histidine (or glutamine in the Asian elephant) residue E7 and the bound O_2 is a conserved feature in mammalian myoglobins and makes a critical contribution to the high oxygen affinity of these molecules (Phillips & Schoenborn, 1981; Bashford et al., 1987). Apolar substitutions at this position in sperm whale myoglobin result in 10−100-fold reductions in O_2 affinity (Rohlfs et al., 1990). Histidine or glutamine is also conserved at the E7 position in vertebrate hemoglobins, although its role may be more complex. In the α-subunits of R-state human hemoglobin, the effects of apolar substitutions at the E7 position are similar to the effects seen in myoglobin; in the β-subunits, substitution of histidine-E7 by glycine or phenylalanine leaves the O_2 affinity unchanged (Mathews et al., 1989).

In the invertebrate kingdom, distal groups at the E7 position capable of donating a hydrogen bond to the oxygen ligand are not as well-conserved. In some cases, the absence of such a residue is accompanied by low O_2 affinity, but in

[†] This work was supported by Grant GR/H68864 from the Science and Engineering Research Council, U.K. (A.J.W.), British Council Travel Grant WAR/922/015 (S.K.), United States Health Service Grants GM-35649 and HL-47020 (J.S.O.), and Grant C-612 from the Robert A. Welch Foundation and the W. M. Keck Foundation (J.S.O.) and in part by grants to M.B. from MURST (40% live protein). C.T.A. is the recipient of a fellowship from the Fondazione A. Buzzati Traverso.

[‡] The coordinates and structure factors associated with the three pig myoglobin mutant crystal structures reported in this manuscript have been deposited at Brookhaven National Laboratories, Upton, Long Island, NY 11973. The identification codes are 1 mnh (H64V-T67R), 1 mnj (H64V-V68I), and 1 mnk (H64V-V68T).

[⊗] Abstract published in *Advance ACS Abstracts,* June 15, 1995.

0006-2960/95/0434-8715$09.00/0 © 1995 American Chemical Society

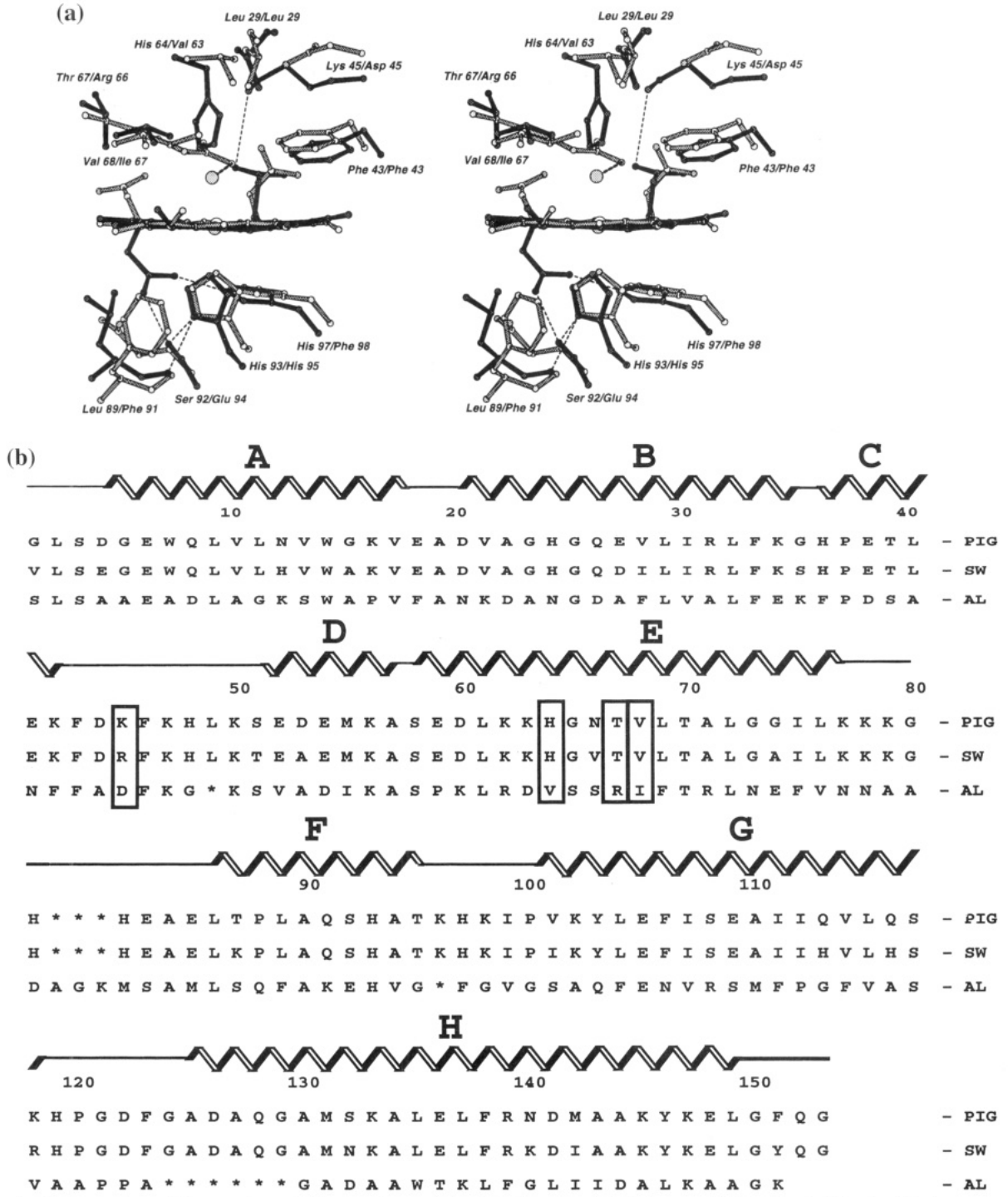

FIGURE 1: (a) Stereoview of the overlapped distal pockets of pig (bold lines) and *Aplysia* myoglobins (shaded lines). The heme group and surrounding residues were picked and displayed in the program QUANTA, and an overlap was performed on selected atoms of the heme groups. The coordinates are those of the fluoride derivative of *Aplysia* myoglobin (Bolognesi et al., 1990) and the aquomet form of pig myoglobin (1 myg). The figure labels indicate the pig residues followed by the *Aplysia* residues. (b) Overlap of the amino acid sequences of *A. limacina* (AL) myoglobin (F. Cutruzzolá, C. Travaglini Allocatelli, A. Brancaccio, and M. Brunori, manuscript in preparation) with those of the pig and sperm whale (SW) proteins. The alignment maximizes the overlap of residues which are topologically equivalent and which are most highly conserved within the globin family (Bashford et al., 1987). The location and extents of the eight α-helices (A-H) in sperm whale myoglobin are shown. The boxed positions CD3, E7, E10, and E11 represent the sites where mutations were introduced in this study.

others it is not. Clearly within the framework of the globin fold there are alternative mechanisms for stabilizing bound oxygen. The structure of myoglobin from the Mediterranean mollusc *Aplysia limacina* (hereinafter *Aplysia*) has a similar fold to that of the mammalian myoglobins, although sequence changes within the distal heme pocket result in quite different stereochemistry and polarity as can be seen from Figure 1 (Bolognesi et al., 1989, 1990). In *Aplysia* myoglobin the E7 residue is valine. Despite the absence of a hydrogen-bonding group at this position, *Aplysia* myoglobin possesses an oxygen affinity that is only 5-fold lower than that of the mammalian myoglobins and some 20-fold higher than the H64V sperm whale myoglobin mutant (Springer et al., 1989; Rohlfs et al., 1990). In the crystal structure of ferric *Aplysia* myoglobin at pH 7.0, the sixth coordination position at the heme iron is not occupied by a water molecule, consistent

Table 1: X-ray Data Collection and Processing Statistics

parameter	H64V-T67R	H64V-V68I	H64V-V68T
space group	$P2_12_12$	$I2_1$[a]	$I2_1$[a]
cell dimensions	$a = 29.7$ Å, $b = 119.5$ Å, $c = 58.2$ Å	$a = 124.3$ Å, $b = 42.6$ Å, $c = 92.5$ Å, $\beta = 92.7°$	$a = 125.3$ Å, $b = 42.5$ Å, $c = 92.4$ Å, $\beta = 92.3°$
d_{min} (Å)	2.3	2.2	2.2
no. of refltns	9174	21 170	23 497
completeness (%)	94.2	85.0	94.5
mean $I/\sigma(I)$	6.7	11.5	5.4
mean obsvtns/refltns	3.5	3.5	4.7
R_{merge}[b] (%) all data	7.0	4.6	8.8
highest resoltn shell	8.4	14.7	16.7

[a] For convenience, we chose to process the data in the nonstandard space group $I2_1$ in which the β-angle is close to 90°, rather than to process the data in a C2 cell in which $\beta \sim 128°$ and $c \sim 157$ Å. [b] $R_{merge} = \Sigma|I_i - I_n|/\Sigma I_n$ where I_i is an observed intensity, hkl, and I_n is the average of the observed equivalents.

with the absence of a polar group at E7 (Bolognesi et al., 1989). In several derivatives of *Aplysia* ferrimyoglobin, the side chain of arginine-E10, which appears to be disordered in the unliganded structure, is folded back into the heme pocket so that the guanidinium group makes favorable interactions with the ligand (Conti et al., 1993). This is consistent with results from NMR studies of the cyanomet derivatives of myoglobins from *Aplysia* and *Dolabella auricularia* which also has a valine at the E7 position (Qin et al., 1992; Yamamoto et al., 1992). If arginine-E10 adopts a similar conformation in the ferrous oxy complex of these mollusc myoglobins, it could compensate for the absence of the distal histidine by forming a hydrogen bond with bound oxygen.

Brunori, La Mar, and co-workers have previously suggested that arginine at the E10 position can stabilize anionic ligands in sperm whale myoglobin mutants lacking the distal histidine. Their ^{1}H NMR data indicate that there is a hydrogen bond formed between arginine-E10 and bound cyanide (Cutruzzolá et al., 1991; Travaglini Allocatelli et al., 1993). In the current study, we have used an extended set of site-directed mutants to explore further the basis of O_2 stabilization and CO discrimination within the framework of the sperm whale and pig myoglobin heme pockets. Starting with distal pocket mutants in which the histidine has been substituted by valine, we have investigated whether mutations introduced singly or in combination at positions CD3, E10, and E11 are able to compensate for the absence of a hydrogen-bonding group at E7 and restore high O_2 affinity. In the process, we sought to simulate the *Aplysia* myoglobin distal heme pocket within the framework of mammalian myoglobin. In *Aplysia* myoglobin, residues CD3, E7, E10, and E11 are Asp, Val, Arg, and Ile, respectively (Figure 1). We have also measured azide binding to the ferric forms of the mutants. Azide binding has been shown to be a sensitive probe of distal pocket stereochemistry and polarity providing data which are complementary to those derived from the O_2 kinetics. The binding of both ligands involves displacement of a water molecule from the distal pocket, and both ligands can be stabilized by positive dipoles in the heme pocket (Brancaccio et al., 1994). Finally, we have determined the crystal structures of the met forms of three of the pig myoglobin double mutants which allow interpretation of the kinetic data in terms of polar and steric influences.

MATERIALS AND METHODS

Preparation of Mutant Proteins. The pig and sperm whale myoglobin mutants were constructed, expressed, and purified as described previously (Dodson et al., 1988; Carver et al., 1991; Travaglini Allocatelli et al., 1993; Cutruzzolá et al., 1991; Springer et al., 1989).

Kinetic Measurements. Overall association and dissociation rate constants for oxygen and carbon monoxide were measured using stopped-flow and conventional flash photolysis techniques as described by Rohlfs et al. (1990). Equilibrium constants were calculated from the ratio of the rate constants. Azide association rates were measured in stopped-flow experiments in which metmyoglobins were mixed with azide solutions of varying concentrations. When the azide association rates were too fast to be measured by rapid mixing techniques, temperature jump kinetic methods were used as described in Brancaccio et al. (1994). Dissociation rates were determined by measuring the rate of ligand displacement by cyanide following the rapid mixing of azidomyoglobin and cyanide solutions as described by Brancaccio et al. (1994).

Crystallography. Crystals of the pig H64V-V68I and H64V-V68T metmyoglobin double mutants were grown in hanging drops from 50 mM phosphate buffer, pH 7.1, and 70−80% ammonium sulfate. These crystals were isomorphous with those of wild type pig myoglobin. The H64V-T67R metmyoglobin did not give crystals under these conditions but yielded crystals in space group $P2_12_12$ when ammonium sulfate was replaced by ammonium phosphate. Because of the high rates of autooxidation of the H64V mutants [Brancaccio et al. (1994) and unpublished observations], X-ray data were recorded from the ferric forms. It has been observed that the heme pocket structures of the deoxy (ferrous) and met (ferric) forms of wild type and a large number of mutant myoglobins are closely similar at neutral pH (Cameron et al., 1993; Quillin et al., 1993, 1995). In view of these similarities, the effects of mutations on the kinetics of binding of ferrous ligands may reasonably be interpreted in terms of alterations in the structures of the corresponding ferric forms.

Crystals were exposed to X-rays generated from a rotating copper anode source, and diffraction intensities were recorded on a Rigaku R-axis II imaging plate. Data were processed with the DENZO package of programs (Z. Otwinowski, Yale University). The details of the data processing are presented in Table 1. The H64V-T67R structure was solved by molecular replacement using as a starting model the coor-

Table 2: Details of the Refined Structural Models

parameter	H64V-T67R	H64V-V68I	H64V-V68T
no. of protein atoms (molecules/au)	1241 (1)	2462 (2)	2446 (2)
no. of waters	116	176	205
R_{cryst}[a] (%)	18.5	16.2	16.4
free R_{cryst} (%)	25.1	24.0	23.7
range of spacing (Å)	10−2.3	10−2.2	10−2.2
rms_{bond} (Å)	0.014	0.019	0.017
rms_{angle} (Å)	0.045	0.059	0.056
rms_{planes} (Å)	0.013	0.014	0.015
missing residues	none	Q152B, G153B	Q152A, G153A, Q152B, G153B
average B-value (Å^2)			
main chain	18.0	25.3	22.1
side chain	28.1	33.2	30.3
solvent	40.2	52.2	52.6

[a] $R_{cryst} = \sum_{hkl}||F_{obs}| - |F_{calc}||/\sum_{hkl}|F_{obs}|$ where $|F_{obs}|$ and $|F_{calc}|$ are the observed and calculated structure factor amplitudes of a reflection, *hkl*, respectively.

dinates for the A molecule of recombinant wild type pig myoglobin (1 myg). The programs ALMN and TFSGEN from the CCP4 suite of programs were used to solve the rotation and translation functions, respectively (CCP4, 1994). The initial R-factor (10−4.0 Å) of 45.3% dropped to 41.4% following rigid body refinement in XPLOR (Brünger, 1990); 10% of the data were set aside for cross-validation analysis (Brünger, 1992). The starting model for the refinement of the H64V-V68I and H64V-V68T mutants was the wild type metmyoglobin structure (1 myg) from which water molecules were removed and mutated side chains truncated. Initially, cycles of rigid body refinement were carried out as described by Derewenda (1989). In the two cases this lowered the R_{cryst} from ~36% to ~30%. Cycles of least-squares refinement in the program PROLSQ reduced the R-values to approximately 22%, at which point $2F_o - F_c$ and $F_o - F_c$ electron density maps were calculated and displayed graphically using the program O (Jones & Kjeldgaard, 1991). This allowed the side chains of the mutated residues to be fitted. Subsequently the models were refined in (i) cycles of the automated refinement procedure using the program ARP in which waters were added to the model (Lamzin & Wilson, 1993), (ii) cycles of the least-squares refinement procedures in PROLSQ (CCP4, 1994), and (iii) sessions of manual model building in the program O (Jones & Kjeldgaard, 1991). The details of the refined structures are presented in Table 2.

RESULTS

O_2 and CO Binding

Substitution of Histidine^{64} by Valine. A key feature of *Aplysia* myoglobin is the replacement of histidine at the E7 position with valine. As may be seen from Table 3, the H64V mutation in pig myoglobin leads to dramatic loss of O_2 affinity and a modest increase in CO affinity as was observed for the same substitution in sperm whale myoglobin (Springer et al., 1989). A detailed characterization of these and related mutants suggests that the imidazole group of the distal histidine lowers the affinity of myoglobin for ligands by stabilizing noncoordinated water in deoxymyoglobin, which must be displaced upon ligand binding. In the case of O_2, this destabilizing influence is offset by a strong hydrogen bond formed between the imidazole side chain and the coordinated oxygen which is polar (Quillin et al., 1993; Springer et al., 1994).

In subsequent experiments, we have used the H64V single mutant as a base line from which to determine whether second- and third-site replacements at topological positions E10 (T67R), E11 (V68I and V68T), and CD3 (R45D) are able to restore the high oxygen affinity of wild type pig and sperm whale myoglobins. These experiments represent, in part, attempts to reshape the heme pocket structure of pig and sperm whale myoglobins to resemble that of *Aplysia* myoglobin and to simulate the ligand binding behavior of the mollusc protein. At the same time, it is possible to examine the effects of individual substitutions in the context of different heme pocket structures and to evaluate the interactions among the residues adjacent to bound ligands.

Substitution of Threonine^{67} by Arginine. The T67R substitution introduces a positively charged group in the region of the solvent-exposed face of the heme. It also removes a γ-methyl from the E10 side chain. Among the mammalian myoglobins, this β-substituent group is largely conserved as part of either a threonine residue as in sperm whale and pig myoglobins or a valine residue as in dog myoglobin. Arg^{67} has no significant effect on the rate or equilibrium parameters for the binding of oxygen or carbon monoxide to myoglobin in the presence of E7 histidine (Table 3). Similarly, only small changes in ligand-binding parameters are observed for T67A, T67V, and T67E substitutions. These results are analogous to the small effects observed for replacements of Lys/Arg^{45} (CD3), which is also situated on the solvent exposed face of the heme pocket (Carver et al., 1991).

The double mutant H64V-T67R was constructed in pig and sperm whale myoglobin, to test whether arginine-E10 can act to stabilize ligands in the absence of the distal histidine residue. Arginine has a flexible side chain, and modeling suggests that the guanidino group of arginine-E10 can interact directly with bound ligands in mammalian myoglobins in the manner suggested for the *Aplysia* protein (Conti et al., 1993; Figure 1a). The presence of arginine^{67} in H64V-T67R does stabilize bound O_2 3−4-fold relative to the H64V single mutant. Since the T67R mutation has no effect on the wild type protein, it seems that the arginine side chain may interact directly with the bound ligand in the oxy form of the double mutant. However, the effect is not dramatic, and K_{O_2} remains 5−10 lower than that observed for *Aplysia* myoglobin.

The heme pocket in the crystal structure of the aquomet form of the pig H64V-T67R mutant is shown in Figure 2. As expected, there is no water at the sixth coordination position at the iron, and the iron is displaced from the plane of the pyrrole nitrogens toward the proximal side. The arginine^{67} side chain is not defined by the electron density beyond Cβ, and it is assumed to be disordered. We have therefore built the preferred arginine conformer into the model at this position. Although arginine^{67} changes the crystallization properties of pig myoglobin, the arginine side chain itself is not involved in crystal contacts. The structure of the pig H64V-T67R mutant is compared with the previously determined structures of the sperm whale H64V-T67R mutant and *Aplysia* myoglobin in Figure 3 (Rizzi et al., 1993; Bolognesi et al., 1989). The figure shows that the E10 Cα carbons have similar positions relative to the heme group. Therefore it is likely that the guanidino group

Table 3: Kinetic Parameters for CO and O_2 Binding to Position 45, 64, 67, and 68 Mutants of Pig and Sperm Whale Myoglobins

protein	k'_{O_2} (μM^{-1} s^{-1})	k_{O_2} (s^{-1})	K_{O_2} (μM^{-1})	k'_{CO} (μM^{-1} s^{-1})	k_{CO} (s^{-1})	K_{CO} (μM^{-1})	M[a]
pig	17	14	1.2	0.78	0.020	39	33
sperm whale	17	16	1.1	0.51	0.019	27	25
Aplysia limacina[b]	15	70	0.21	0.50	0.02	25	120
			Single Mutants				
H64V (pig)	110	10 000	0.011	6.4	0.050	130	12 000
H64V (SW)[c]	110	9900	0.011	7.1	0.056	130	12 000
T67R (pig)	17	15	1.1	0.75	0.019	42	38
T67R (SW)	17	11	1.5	0.56	0.018	31	21
T67E (pig)	21	8.9	2.4	1.5	0.018	84	35
T67A (pig)	19	7.8	2.4	1.6	0.018	89	37
T67V (pig)	22	12	1.8	1.1	0.022	50	28
V68I (pig)	1.7	14	0.12	0.045	0.027	1.7	14
V68I (SW)[d]	3.2	14	0.23	0.050	0.024	2.1	9
V68T (pig)[e]	2.8	39	0.072	0.61	0.079	7.7	110
			Double Mutants				
H64V-T67R (pig)	81	2900	0.028	7.1	0.038	190	6800
H64V-T67R (SW)	98	2300	0.043	12	0.038	320	7400
H64V-V68I (pig)	4.2	1600	0.0026	0.045	0.045	1.0	390
H64V-V68T (pig)[f]	100	4000	0.025	27	0.063	430	17 200
			Triple Mutants				
H64V-T67R-V68I (pig)	2.5	420	0.0060	0.053	0.035	1.5	250
R45D-H64V-T67R (SW)	88	2300	0.039	7.2	0.050	144	3700

[a] $M = K_{CO}/K_{O_2}$. [b] Taken from Wittenberg et al. (1965, 1972). [c] Data from Springer et al. (1989). The rates for the H64V mutant presented in Springer et al. (1989) and Rohlfs et al. (1990) have been corrected (Quillin et al., 1993). [d] Data from Egeberg et al. (1990). [e] Data from Smerdon et al. (1991). [f] Data from Cameron et al. (1993).

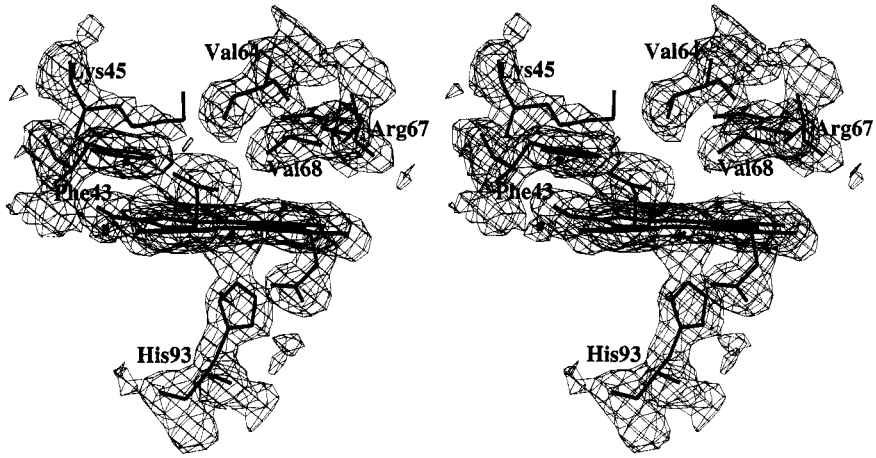

FIGURE 2: Stereorepresentation of the met form of the pig H64V-T67R crystal structure in the region of the heme pocket showing lysine[45] and arginine[67] at the entrance to the pocket, phenylalanine[43], valine[64], and valine[68] in the distal pocket, and histidine[93] on the proximal side of the heme. The associated $2F_o - F_c$ electron density is contoured at 1 standard deviation above the average electron density of the map. It is apparent that there is disorder of the lysine[45] and arginine[67] side chains. No electron density associated with coordinated water is observed, and the iron resides out of the heme plane on the proximal side.

of the E10 side chain can explore the same conformational space in the three structures. However, the valine-E7 side chain is ~1 Å closer to the plane of the heme group in the double mutants relative to the *Aplysia* protein, so that rotation of the arginine[67] side chain into the heme pocket may be more restricted in the mammalian myoglobin mutants.

Substitution of Arginine[45] by Aspartate. It was pointed out in an earlier study (Cutruzzolá et al., 1991) that the presence of arginine at the CD3 position in sperm whale myoglobin may restrict the conformational freedom of arginine-E10 and hinder its interaction with bound ligands through a mutual electrostatic repulsion. Lysine-CD3 in pig myoglobin may cause similar complications. By contrast, residue CD3 in *Aplysia* myoglobin is aspartate. To test the hypothesis that the function of arginine[67] is dependent on the nature of the residue at CD3, a triple mutant of sperm whale myoglobin was constructed, R45D-H64V-T67R. Kinetic analysis of this mutant shows however that its oxygen-binding characteristics are very similar to those of the H64V-T67R double mutant (Table 3; Travaglini Allocatelli et al., 1993).

Substitution of Valine[68] by Isoleucine. Valine[68] (E11) lies in van der Waals contact distance both of bound ligands and of the imidazole group of the distal histidine in mammalian myoglobins. The δ-methyl group introduced in the single V68I mutant of sperm whale deoxymyoglobin resides directly above the iron and hinders ligand binding (Quillin et al., 1995). The V68I substitution in pig myoglobin causes a 10-fold reduction in the rate constant for oxygen binding and a 17-fold reduction in that for CO binding; the dissociation rates are little affected by the introduction of the δ-methyl group so that the affinity of the protein is 10-fold lower for O_2 and 22-fold lower for CO. The V68I replacement in sperm whale myoglobin causes similar lowering of

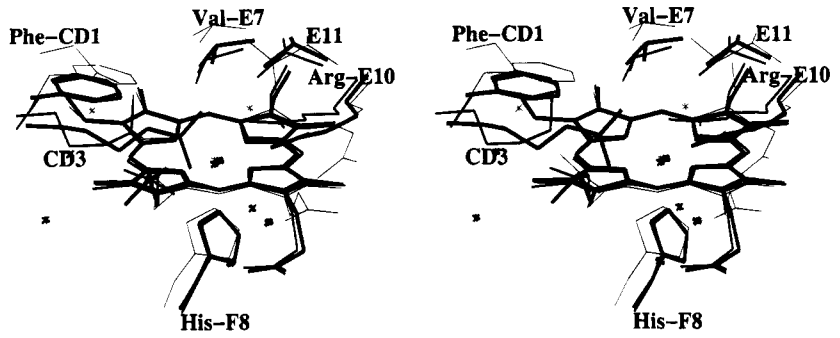

FIGURE 3: Stereorepresentation of the crystal structures of the met forms of *Aplysia* myoglobin (thin lines), the pig H64V-T67R mutant myoglobin (lines of intermediate thickness), and the sperm whale H64V-T67R mutant myoglobin (thick lines) (Rizzi et al., 1993). The structures were overlapped on the atoms of the heme group, excluding the propionic acid groups, using a least-squares minimization procedure. For the pig structure, the A molecule of the asymmetric unit is shown. It is apparent that the Val-E7 side chain is closer to the heme plane in the pig and sperm whale H64V-T67R mutants than in the *Aplysia* myoglobin; the Cβ(E7)−CHA(heme) distances are 6.1, 6.5, and 7.3 Å, respectively.

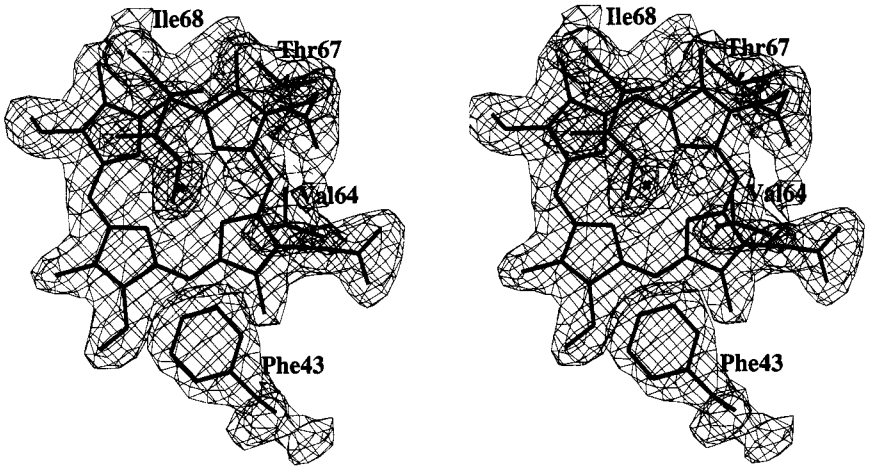

FIGURE 4: Stereoview of the structure of the heme and distal pocket of the pig H64V-V68I metmyoglobin. The view is approximately orthogonal to the heme plane and shows the positions of the distal residues Phe^{43}, Val^{64}, Thr^{67}, and Ile^{68}. The associated $2F_o - F_c$ electron density is contoured at 1.6 standard deviations above the average electron density of the map. The Cδ methyl group of isoleucine^{68} resides directly above the iron atom.

the association rate and equilibrium constants though the effects are 2-fold smaller (Table 3; Egeberg et al., 1990).

For the H64V-V68I double mutant, the isoleucine substitution clearly has the dominant effect on the association rate processes. Valine^{64} alone causes 6−8-fold increases in the association rate constants, whereas isoleucine^{68} alone reduces the same parameters by 10−20-fold with respect to wild type myoglobin. In the double mutant, k'_{O_2} is 4-fold lower and k'_{CO} is 17-fold lower than for the wild type protein. In contrast, the valine^{64} substitution exerts the dominant effect on the dissociation rates with k_{O_2} ~120 higher and k_{CO} 2-fold higher in the H64V-V68I mutant relative to the wild type protein. As a result, the association equilibrium constants for O_2 and CO binding to the double mutant are extremely low: 0.0026 μM^{-1} for O_2 and 1 μM^{-1} for CO, among the lowest for any myoglobin mutant studied (Springer et al., 1994).

Figure 4 shows the crystal structure of the met form of the H64V-V68I pig double mutant in the vicinity of the heme group and confirms that the Cδ group of the isoleucine side chain is located immediately above the iron in a position that will severely sterically hinder the binding of ligands. The distal heme pocket is very nonpolar, and as a result no water is coordinated to the iron in the met form.

The kinetic data for the H64V-T67R-V68I triple mutant reinforce the conclusions derived from the H64V-V68I and H64V-T67R analyses (Table 3). The isoleucine substitution causes marked decreases in the association rate constants for both ligands regardless of the residues at E7 and E10. The O_2 affinity of the triple mutant is 2−3-fold greater than that of the H64V-V68I double mutant showing again that Arg^{67} is able to stabilize bound oxygen in the absence of the distal histidine.

Substitution of Valine^{68} by Threonine. The V68T single mutant of pig myoglobin was originally constructed as a strategy for increasing O_2 affinity by placing a second hydrogen bond donor group adjacent to the bound ligand (Smerdon et al., 1991). Studies with this mutant, however, showed that its affinity for all ligands was lowered and K_{O_2} decreased by a factor of 17. The crystal structure of V68T deoxymyoglobin shows that the noncovalently bound distal pocket water molecule is stabilized by hydrogen bonding to the threonine^{68} hydroxyl group as well as to N_ϵ-H of the distal histidine (Cameron et al., 1993). As a result, water displacement is more difficult and the rate of O_2 association is lowered. The hydroxyl of the threonine also donates a hydrogen bond to >C=O of histidine^{64} so that its nonbonding electrons are oriented toward the ligand. This partial negative charge interacts unfavorably with bound O_2, increasing k_{O_2} and lowering K_{O_2}.

Threonine^{68} has quite different effects after histidine^{64} has been replaced by valine (Table 3). The affinity of H64V-

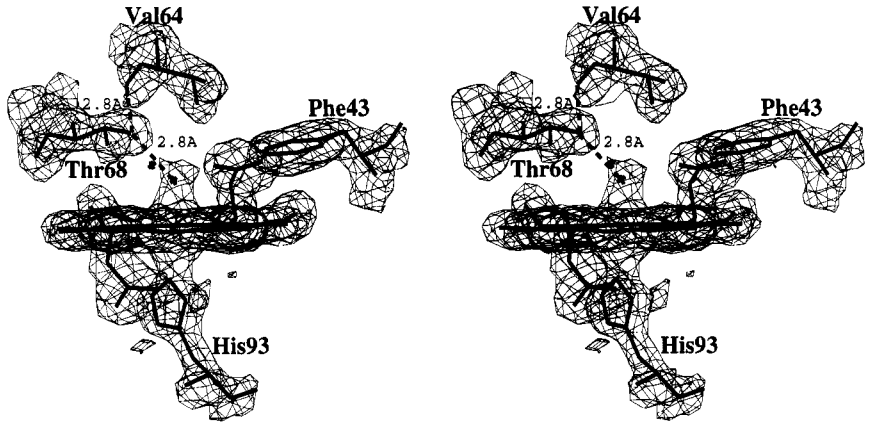

FIGURE 5: Stereoview of the crystal structure of the met form of the pig H64V-V68T myoglobin in the vicinity of the heme group. The view is from the back of the heme pocket and includes the heme group, Phe[43], Val[64], Thr[68], and His[93]. The $2F_o - F_c$ electron density associated with the structure is contoured at 1.5 standard deviations above the mean electron density of the map. There is clear evidence for a water molecule at the sixth coordination position. The dashed lines indicate possible hydrogen-bonding interactions of the -OH group of threonine.[68]

V68T for both O_2 and CO is higher by a factor of 2−3 than in the H64V single mutant. For O_2 this arises from a lowering of the dissociation rate constant implying that the presence of the threonine -OH group stabilizes bound oxygen. For CO the higher affinity arises predominantly from an unusually high association rate constant, 27 μM^{-1} s^{-1}, as high as that of k'_{CO} for the Leu[64] mutant of sperm whale myoglobin (Rohlfs et al., 1990). In the valine[64] background, the V68T mutation no longer lowers the rate constant for O_2 association.

The crystal structure of the H64V-V68T pig double mutant has been determined and is shown in the environment of the heme group in Figure 5. The iron is six-coordinate in the met form with clear electron density for a coordinated water ligand in the distal pocket. This water molecule is stabilized by donation of a hydrogen atom to the nonbonded electrons of the hydroxyl group of threonine[68]. As was seen in the crystal structure of the aquomet form of the V68T single mutant, the threonine[68] hydroxyl group is in a position to form a strong hydrogen bond with the main chain >C=O of histidine[64], the -OH···O=C< distance being 2.8 Å. The structure shows that the distal pocket is accessible and more polar than that of the H64V single mutant of sperm whale myoglobin (Quillin et al., 1993). A water molecule has been placed in an $F_o - F_c$ electron density peak located along a channel connecting threonine[68] with the solvent-exposed edge of the heme group. No such density is seen in the H64V-V68I or H64V-T67R structures.

Azide Binding. Measurements of the rate constants for azide binding to the ferric form of myoglobin have proved to be a sensitive probe of distal pocket structure and provide information that complements the analysis of oxygen binding to the ferrous forms (Brancaccio et al., 1994). O_2 and azide binding each involve displacement of a distal pocket water molecule, albeit a coordinated water in the latter case. Similarly both bound ligands have anionic character and are stabilized by positive dipoles or hydrogen bond donors.

Table 4 presents the kinetic parameters for azide binding to the ferric forms of *Aplysia*, sperm whale, and pig myoglobins and a number of mutants. Removal of the imidazole group in the H64V mutant causes 50−100-fold increases in k'_{N_3}, and the crystal structures of the H64V metmyoglobin mutants reveal a less sterically hindered distal

Table 4. Kinetic Parameters for the Binding of Azide to Position 64, 67, and 68 Mutants of Pig and Sperm Whale Myoglobins

protein	k'_{N_3} (mM^{-1} s^{-1})	k_{N_3} (s^{-1})	K_{N_3} (mM^{-1})	T (°C)
Aplysia[a]	1,800	750	2.5	25
pig[b]	9.8	0.18	54	20
sperm whale[b]	2.9	0.10	29	20
H64V (pig)[b]	360	500	0.72	20
H64V (SW)[b]	260	740	0.35	25
T67R (pig)[b]	26	0.13	200	20
T67R (SW)[b]	7	0.06	120	20
V68I (SW)[b]	64	8	8	20
V68T (pig)[b]	0.13	1.2	0.11	20
H64V-T67R (pig)	460	130	3.6	25
H64V-T67R (SW)[c]	300	48	6.3	25
H64V-V68I (pig)	15	27	0.55	20
H64V-V68T (pig)	16	29	0.55	20
H64V-T67R-V68I (pig)	180	1700	0.1	25

[a] Wittenberg et al. (1965, 1972). [b] Brancaccio et al. (1994). [c] Cutruzzolá et al. (1991).

pocket in which no coordinated water is present (Brancaccio et al. 1994; Quillin et al., 1993; A.J.W. unpublished observations). The loss of the stabilizing hydrogen-bonding interaction between the imidazole side chain and the bound azide ligand results in a 1000−7000-fold increase in k_{N_3} and a net 50−100-fold decrease in affinity.

In contrast to its behavior toward the ferrous ligands, arginine[67] does have a significant effect on the rate and equilibrium parameters for azide binding to pig and sperm whale myoglobins. As discussed by Brancaccio et al. (1994), positive charges at the entrance to the heme pocket facilitate diffusion of the anion into the protein and stabilize the bound ligand. The arginine-E10 replacement in the H64V background increases K_{N_3} by a factor of 18 in sperm whale myoglobin and by a factor of 5 in the pig protein.

The V68I substitution has curious effects on azide binding. In the wild type background, this mutation increases the association and dissociation rate constants 22- and 80-fold, respectively. In the Val[64] background, opposite effects are observed; k'_{N_3} and k_{N_3} are lowered 24- and 19-fold, respectively, in the H64V-V68I double mutant compared to the H64V single mutant. The effects of threonine[68] on azide binding are also markedly sensitive to the nature of residue 64. In the presence of histidine[64], threonine[68] increases the azide dissociation rate constant 7-fold and lowers the affinity

Table 5: Effects of T67R, V68I, and V68T Mutations on O_2, CO, and N_3^- Binding to Myoglobin in the Presence and Absence of the Distal Histidine[a]

mutation	genetic background	O_2 binding $\delta\Delta G^{\ddagger}$ assoc	O_2 binding $\delta\Delta G^{\ddagger}$ dissoc	O_2 binding $\delta\Delta G°$ equil	CO binding $\delta\Delta G^{\ddagger}$ assoc	CO binding $\delta\Delta G^{\ddagger}$ dissoc	CO binding $\delta\Delta G°$ equil	azide binding $\delta\Delta G^{\ddagger}$ assoc	azide binding $\delta\Delta G^{\ddagger}$ dissoc	azide binding $\delta\Delta G°$ equil
His^{64} to Val	pig (WT)	−1.09	−3.83	2.73	−1.23	−0.53	−0.70	−2.10	−4.62	2.51
His^{64} to Val	SW (WT)	−1.09	−3.74	2.68	−1.53	−0.63	−0.92	−2.66[b]	−5.27[b]	2.61[b]
Thr^{67} to Arg	pig (WT)	0.00	−0.04	0.05	0.02	0.05	−0.04	−0.57	0.19	−0.76
Thr^{67} to Arg	SW (WT)	0.00	0.22	−0.18	−0.05	0.03	−0.08	−0.51	0.30	−0.83
Thr^{67} to Arg	pig (Val^{64})	0.18	0.72	−0.54	−0.06	0.16	−0.22	−0.15[b]	0.80[b]	−0.95[b]
Thr^{67} to Arg	SW (Val^{64})	0.07	0.85	−0.79	−0.31	0.23	−0.52	−0.08[c]	1.62[c]	−1.71[c]
Thr^{67} to Arg	pig (Val^{64}-Ile^{68})	0.30	0.78	−0.49	−0.10	0.15	−0.24			
Val^{68} to Ile	pig (WT)	1.34	0.00	1.34	1.66	−0.17	1.82			
Val^{68} to Ile	SW (WT)	0.97	0.08	0.91	1.35	−0.14	1.49	−1.80	−2.55	0.75
Val^{68} to Ile	pig (Val^{64})	1.90	1.07	0.83	2.89	0.06	2.83	1.85	1.70	0.16
Val^{68} to Ile	SW (Val^{64}-Arg^{67})	2.03	1.12	0.89	2.85	0.05	2.82			
Val^{68} to Thr	pig (WT)	1.05	−0.60	1.64	0.14	−0.80	0.94	2.52	−1.10	3.61
Val^{68} to Thr	pig (Val^{64})	0.06	0.53	−0.48	−0.84	−0.13	−0.70	1.80	1.66	0.16

[a] In kcal/mol and calculated at 20 °C unless otherwise stated. [b] The mutant and background parameters in eq 1 were measured at two different temperatures, 20 and 25 °C (Table 4). In calculating $\delta\Delta G$, a T of 25 °C (298 K) was used. [c] Calculated at 25 °C.

500-fold, whereas when valine is at position 64, the same mutation lowers k_{N_3} ~20-fold and the azide affinity less than 2-fold.

DISCUSSION

Free Energy Considerations. For the purposes of comparing substitutions in different genetic backgrounds and to evaluate whether the effects of pairs of mutations are coupled, it is convenient to discuss the ligand-binding data in terms of free energy changes. These have been calculated for the association equilibrium constants and the association and dissociation rate constants according to eq 1. These values are presented for O_2, CO, and N_3^- in Table 5.

$$\delta\Delta G = -RT \ln(\text{mutant parameter/background parameter}) \quad (1)$$

Effects of H64V. It is seen from Table 5 that the $histidine^{64}$ to valine substitution in wild type pig and sperm whale myoglobins lowers the overall kinetic barriers to ligand binding for both O_2 and CO and makes the free energy change for O_2 binding more positive and that for CO binding more negative. The lower barrier to ligand association results from destabilization of the water molecule that resides in the distal pocket in wild type deoxymyoglobin and is displaced upon ligand binding (Quillin et al., 1993). Destabilization of the distal pocket water inherently increases ligand affinity so that the MbCO complex is stabilized by −0.7 and −0.9 kcal/mol. For bound O_2, the loss of the hydrogen bond to N_ϵ-H of the distal histidine offsets this gain, and as a result K_{O_2} decreases markedly.

Azide binding also requires displacement of water, in this case an H_2O molecule coordinated to the ferric iron atom in aquometmyoglobin. In wild type pig and sperm whale myoglobins, substitution of $histidine^{64}$ by valine substantially lowers the kinetic barriers to ligand association due to removal of both coordinated water and steric hindrance by the distal histidine. The dominant factor determining azide-binding rates is steric hindrance by the imidazole side chain which acts as a gate regulating a polar channel from the bulk solvent into the heme pocket (Brancaccio et al., 1994). As well as inhibiting the rate of association, His^{64} forms a strong hydrogen bond with the bound azide. The loss of this bond in the H64V single mutants dramatically lowers the barrier to ligand escape by ~5 kcal/mol. It is interesting to note that the H64V substitution produces similar effects on the parameters for O_2 and N_3^- binding (Table 5).

Effects of T67R. Introduction of the T67R mutation has essentially no effect on the kinetic barriers and the equilibrium states for the binding of O_2 and CO when histidine is at position 64 (Table 5). When valine is at position 64, however, the bound oxygen is stabilized by ~−0.6 kcal/mol. These data are consistent with the arginine swinging into the distal pocket to interact favorably with bound oxygen, an interaction that can only occur in the absence of the distal histidine. The contribution of this interaction in mammalian myoglobins is, however, modest; the O_2 affinity of H64V-T67R myoglobin is lower than that of *Aplysia* or mammalian myoglobins, and arginine-E10 does not satisfactorily compensate for the 2.7 kcal/mol in binding free energy lost upon substitution of histidine-E7 with valine. A plausible explanation is that the valine-E7 side chain is ~1 Å closer to the heme group in the mammalian myoglobin mutants than it is in the mollusc protein, and as a result, there is greater hindrance to interactions between arginine-E10 and bound ligands in the recombinant myoglobins (Figure 3). As shown in Table 5, bound CO is also stabilized to a small extent by arginine-E10 in the H64V background which is consistent with the presence of a positive electrostatic field adjacent to the bound CO (Li et al., 1994). The absence of significant effects on the barriers to ligand entry suggests that $arginine^{67}$ does not stabilize distal pocket water in the deoxy form of the H64V-T67R double mutant. This conclusion is supported by the lack of water coordination to the iron atom in the structure of the ferric form of this double mutant (Figure 2).

The introduction of $arginine^{67}$ increases azide affinity regardless of the residue at position 64. In the His^{64} background, the kinetic barrier to ligand association is selectively lowered, whereas in the Val^{64} background the T67R mutation raises the barrier to ligand dissociation (Table 5). In structural terms, electrostatic attraction of the anion by positively charged residues at the heme periphery lowers

the barrier to azide entry only into the wild type protein, presumably because in the Val[64] mutant this barrier is already lowered to such an extent that it is no longer rate limiting. As in the case of O_2 binding, removal of the distal histidine appears to permit direct, albeit weak, interaction of the positively charged arginine side chain with the bound ligand, raising the barrier to azide dissociation in H64V-T67R metmyoglobin.

Effects of V68I. Table 5 shows that the effects of the V68I substitution on the barriers to ligand association are larger in the Val[64] background than in the His[64] background. Quillin et al. (1995) have shown that isoleucine[68] decreases geminate rebinding of oxygen to the iron from within the distal pocket of V68I myoglobin. The Cδ methyl group of isoleucine lies directly over the iron and sterically hinders ligand binding, raising the overall barrier to ligand association and destabilizing the bound state. However, the crystal structure of the deoxy form of this mutant also shows that isoleucine[68] excludes the non-covalently bound water observed in wild type deoxymyoglobin from the distal pocket. This will have a tendency to compensate partially for the effects of steric hindrance. In the crystal structure of the pig H64V-V68I double mutant, the isoleucine is again observed to reside directly over the iron which again will raise the barrier to ligand association. Here, however, the steric hindrance factor is not offset by a destabilizing influence on distal pocket water, since no water is present in deoxymyoglobin when histidine[64] is replaced by valine. The full inhibitory effect of raising the inner kinetic barrier to O_2 and CO binding is therefore manifested in the overall barrier to ligand association in the Val[64] background (Table 5).

For azide, similar structural considerations can account for the effects of V68I on the association kinetic barrier. Ile[68] both destabilizes coordinated water in the aquomet form and sterically hinders entry of the azide ligand. These two factors oppose each other, and in the wild type protein, the destabilizing effect on the water molecule dominates and the barrier to azide association is lowered. In the Val[64] background, the coordinated water in the metmyoglobin is absent, so the influence of steric hindrance prevails and the overall barrier to azide association is raised by Ile[68] (Table 5).

Effects of V68T. In the presence of His[64], Thr[68] increases the barrier to ligand association, lowers the barrier to dissociation, and increases the free energy for O_2 binding by 1.6 kcal/mol (Table 5). In contrast, when valine is at E7, the V68T substitution decreases ΔG for O_2 binding by −0.5 kcal/mol, by raising the barrier to ligand dissociation and keeping the barrier to ligand association unchanged. For ligand association, these observations imply that in the H64V-V68T mutant ligand binding does not involve a rate-limiting water displacement step, either because no water occupies the distal pocket in the deoxy form or because the water that is present is more easily displaced owing to the absence of the distal histidine.

The influence of Thr[68] on the barrier to oxygen dissociation in the double mutant is harder to rationalize. In the single mutant, we have previously interpreted the destabilizing influence of Thr[68] as arising from unfavorable interactions between the nonbonding orbitals of the hydroxyl oxygen and the electronegative dioxygen ligand. The threonine[68] -OH is positioned 2.5−2.9 Å from the main chain >C=O group of histidine[64] in both the deoxy and met forms of V68T myoglobin, which places restrictions on the hydrogen-bonding interactions that can take place (Cameron et al., 1993; Smerdon et al., 1991). The latter can act only as a hydrogen bond acceptor group, while the -OH group can only donate a single hydrogen bond. As a result, the oxygen of the -OH group will have its nonbonded electron pairs oriented toward the ligand. The same interactions persist in the structure of the met form of the H64V-V68T double mutant. One possible explanation for the increase in K_{O_2} for the H64V-V68T mutant relative to H64V myoglobin would be the presence of a distal pocket water molecule in the liganded form which solvates both the Thr[68] hydroxyl group and the bound oxygen. A similar involvement of distal pocket water accounts for the observation that K_{O_2} for the H64G mutant of sperm whale myoglobin is 4−8-fold higher than those of the H64V and H64L mutants (Quillin et al., 1993).

The V68T mutation raises the kinetic barrier to azide binding regardless of whether histidine or valine is present at position 64. For the V68T single mutant, this observation was interpreted in terms of the threonine -OH providing an additional hydrogen bond to the coordinated water molecule, inhibiting its displacement by ligand. The same explanation applies for the double mutant. In the crystal structure of the met form of H64V-V68T, there is clear electron density for a coordinated water residing within hydrogen-bonding distance of the threonine hydroxyl (Figure 5). The barrier to azide dissociation is lowered in the single mutant but raised in the double mutant, as is observed for O_2 binding to the ferrous form. In the His[64] protein, the orientation of the nonbonded hydroxyl oxygen orbitals will destabilize bound azide in a similar way to the destabilization of bound oxygen described above. In the H64V-V68T protein however, the distal pocket is open and accessible to solvent, and the crystal structure shows that solvent water penetrates the threshold of the heme pocket. The threonine -OH presumably favors entry of water into the pocket which, as in the case of O_2, could dissipate the effects of the threonine dipole and stabilize the bound azide.

Mimicry of Aplysia Myoglobin. Mutations have been introduced in pig and sperm whale myoglobin at four positions singly or in combination in an attempt to mimic the ligand-binding properties of *Aplysia* myoglobin. The question we have attempted to address is how the mollusc protein stabilizes iron-bound oxygen in the absence of a hydrogen bond donor at the E7 position. A number of structural and spectroscopic studies of complexes between *Aplysia* myoglobin and ferric ligands have indicated that arginine-E10 supplies a stabilizing hydrogen bond to the bound ligands. Such an interaction has been directly observed in the X-ray structure of the fluoride complex (Bolognesi et al., 1990). We have been unable to compensate for the drastic effects on ligand binding of the loss of histidine-E7 in the context of pig or sperm whale myoglobin even though some stabilization of O_2 and azide is observed in the H64V-T67R double mutant. An additional substitution at position E11 to make the triple mutant H64V-T67R-V68I serves only to lower the O_2 affinity by a further factor of ~4 causing K_{O_2} to be 30-fold lower than that of the *Aplysia* myoglobin. Substitutions at position CD3 (aspartate in *Aplysia*, lysine/arginine in pig/sperm whale) also have only small effects either alone or in combination with valine-E7

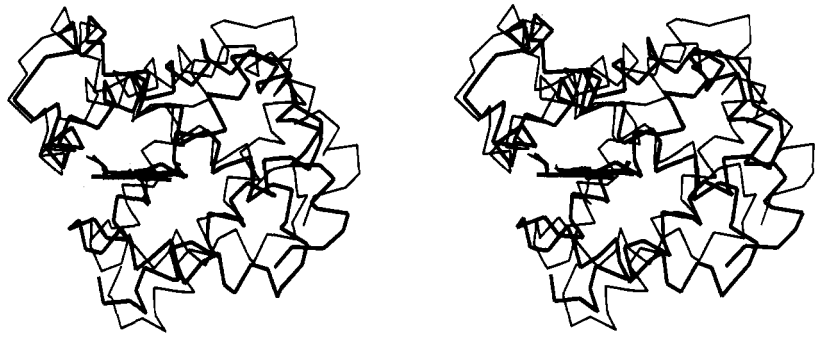

FIGURE 6: Superposition of the Cα atoms of the A molecule of pig H64V-T67R myoglobin (thin lines) with *Aplysia* myoglobin (thick lines). The overlap minimizes the rms difference in the positions of the atoms in the plane of the heme groups in the two molecules.

[Carver et al. (1991) and this study]. It would therefore appear that other, functionally significant differences in primary sequence and/or tertiary structure exist between the mammalian and invertebrate myoglobins. One consequence of these differences is that the side chain of valine-E7 is further displaced from the plane of the heme group in *Aplysia* myoglobin than in the mammalian mutants, which may be critical in permitting the side chain of arginine-E10 to realize potentially favorable interactions with bound oxygen.

Alternatively, observed differences in conformation of the heme 6- and 7-propionate groups may have a direct bearing on the precise conformations of arginine-E10 in *Aplysia* myoglobin and the pig and sperm whale mutant proteins. In the mammalian myoglobins characterized structurally, the 7-propionate group is located on the proximal side of the heme forming a salt-bridging interaction with histidine-FG2. In the mollusc protein, this propionate is often observed to reside on the opposite side of the heme, forming a salt bridge with arginine-E10 which may serve to position the guanidinium group adjacent to bound ligands (Conti et al., 1993; Figure 1a). The relative differences in the propionate positions also led us to consider other, more subtle differences on the proximal side of the respective heme cavities. Smerdon et al. (1993) have shown that perturbation of an extensive hydrogen-bonding lattice involving histidine-F8, histidine-FG2, leucine-F4, and serine-F7 can have significant effects on both heme stability and the affinity of pig myoglobin for ferric and ferrous ligands. Specifically, replacement of serine^{92} (F7) with alanine, valine, or leucine resulted in 2−5-fold increases in O_2 affinity. The X-ray structure of the S92L mutant shows a displacement of the 7-propionate toward the distal side. It is interesting to note that the F7 residue in *Aplysia* myoglobin is glutamic acid and the FG2 residue is phenylalanine (Figure 1). Mutations at F7 or substitutions of histidine-FG2 could, in combination with the mutations at E7, E10, and E11 in pig/sperm whale myoglobin, result in a more authentic, *Aplysia*-like distal heme environment and more closely mimic the remarkable ligand-binding properties of this protein.

General Implications. Attempts to transfer specific functions from a donor protein to a structurally related recipient protein lacking that function represent opportunities to probe possible pathways of protein evolution. For instance, the bicarbonate effect in crocodile hemoglobin and the higher oxygen affinity of the hemoglobins of high-altitude geese have been genetically engineered into human hemoglobin (Komiyama et al., 1995; Jessen et al., 1991). Protein-engineering experiments that involve transplantation of a ligand-binding function, e.g., chimaeric transcription factors and humanized antibodies, can also lead to molecules with potentially advantageous therapeutic properties (Choo et al., 1994; Riechmann et al., 1988).

The results obtained in this study suggest that it is not possible to adapt the mammalian myoglobins to recognize ligands in the manner of *Aplysia* myoglobin with just a small number of substitutions in the heme pocket. This may well be a consequence of the large evolutionary separation of these molecules which is suggested by the low level of sequence identity (Figure 1b). This leads to small but distinct differences in the main chain atomic positions of key residues which impose constraints on the possible side chain stereochemistry in the distal pocket. This is particularly crucial in the globin system because of the enclosed nature of the ligand-binding site and the small size of the ligand. It is also apparent that, within the heme pocket of myoglobin, the effects of pairs of mutations are rarely additive, increasing the complexity of attempts to compensate for the loss of the distal histidine which is already an ambitious undertaking, owing to the dominant effects of this residue on O_2 affinity and resistance to autooxidation (Springer et al., 1994).

Future strategies will need to address whether the origins of the small changes in the relative positions of the main chain atoms of the E-helix relative to the heme can be attributed to a limited number of residue differences elsewhere in the protein. From the point of view of the heme, as shown in Figure 6, the excursion the polypeptide takes between the functionally important E-helix residues (E7−E11) and the invariant His-F8 is noticeably different in the mammalian and mollusc proteins, due in part to a three-residue deletion at the EF corner in mammalian myoglobin (Figure 1b). The angle the F-helix makes with the heme plane and with the E-helix is 5−10° higher in the mammalian proteins than in *Aplysia* myoglobin. In view of the fact that these helices make abundant interactions with the heme, one another, and the core of the protein, adapting the course of the backbone in this region of the protein may require more extensive mutagenesis.

ACKNOWLEDGMENT

We thank Martino Bolognesi for providing the coordinates of the H64V-T67R mutant of sperm whale myoglobin.

REFERENCES

Bashford, D., Chothia, C., & Lesk, A. M. (1987) *J. Mol. Biol. 196*, 199−216.

Bolognesi, M., Onesti, S., Gatti, G., Coda, A., Ascenzi, P., & Brunori, M. (1989) *J. Mol. Biol. 205*, 529−544.

Bolognesi, M., Coda, A., Frigerio, F., Gatti, G., Ascenzi, P., & Brunori, M. (1990) *J. Mol. Biol. 213*, 621−625.
Brancaccio, A., Cutruzzolá, F., Travaglini Allocatelli, C., Brunori, M., Smerdon, S. J., Wilkinson, A. J., Dou, Y., Keenan, D., Ikeda-Saito, M., Brantley, R. E., & Olson, J. S. (1994) *J. Biol. Chem. 260*, 13843−13853.
Brünger, A. T. (1990) X-PLOR Version 2.1, Yale University, New Haven, CT.
Brünger, A. T. (1992) *Nature 355*, 472−475.
Cameron, A. D., Smerdon, S. J., Wilkinson, A. J., Habash, J., Helliwell, J. R., Li, T., & Olson, J. S. (1993) *Biochemistry 32*, 13061−13070.
Carver, T. E., Olson, J. S., Smerdon, S. J., Krzywda, S., Wilkinson, A. J., Gibson, Q. H., Blackmore, R. S., Dezz Ropp, J., & Sligar, S. G. (1991) *Biochemistry 30*, 4697−4705.
CCP4 (1994) *Acta Crystallogr. D50*, 760−763.
Choo, Y., Sánchez-Garcia, I., & Klug, A. (1994) *Nature 372*, 642−645.
Conti, E., Moser, C., Rizzi, M., Mattevi, A., Lionetti, C., Coda, A., Ascenzi, P., Brunori, M., & Bolognesi, M. (1993) *J. Mol. Biol. 233*, 498−508.
Cutruzzolá, F., Travaglini Allocatelli, C., Ascenzi, P., Bolognesi, M., Sligar, S. G., & Brunori, M. (1991) *FEBS Lett. 282*, 281−284.
Derewenda, Z. S. (1989) *Acta Crystallogr. A45*, 227−234.
Dodson, G. G., Hubbard, R. E., Oldfield, T. J., Smerdon, S. J., & Wilkinson, A. J. (1988) *Protein Eng. 2*, 233−237.
Egeberg, K. D., Springer, B. A., Sligar, S. G., Carver, T. E., Rohlfs, R. J., & Olson, J. S. (1990) *J. Biol. Chem. 265*, 11788−11795.
Jessen, T.-H., Weber, R. E., Fermi, G., Tame, J., & Braunitzer, G. (1991) *Proc. Natl. Acad. Sci. U.S.A. 88*, 6519−6522.
Jones, T. A., & Kjeldgaard, M. (1991) in *O-The Manual*, Uppsala University, Sweden.
Komiyama, N. H., Miyazaki, G., Tame, J., & Nagai, K. (1995) *Nature 373*, 244−246.
Lamzin, V., & Wilson, K. S. (1993) *Acta Crystallogr. D49*, 129−147.
Li, T., Quillin, M. L., Phillips, G. N., Jr., & Olson, J. S. (1994) *Biochemistry 33*, 1433−1446.
Mathews, A. J., Rohlfs, R. J., Olson, J. S., Tame, J., Renaud, J.-P., & Nagai, K. (1989) *J. Biol. Chem. 264*, 16573−16583.
Phillips, S. E. V., & Schoenborn, B. P. (1981) *Nature 292*, 81−82.
Qin, J., La Mar, G. N., Ascoli, F., Bolognesi, M., & Brunori, M. (1992) *J. Mol. Biol. 224*, 891−897.
Quillin, M. L., Arduini, R. M., Olson, J. S., & Phillips, G. N., Jr. (1993) *J. Mol. Biol. 234*, 140−155.
Quillin, M. L., Li, T., Olson, J. S., Phillips, G. N., Jr., Dou, Y., Ikeda-Saito, M., Regan, R., Carlson, M., Gibson, Q. H., Li, H., & Elber, R. (1995) *J. Mol. Biol. 245*, 416−436.
Riechmann, L., Clark, M., Waldmann, H., & Winter, G. (1988) *Nature 332*, 323−327.
Rizzi, M., Bolognesi, M., Coda, A., Cutruzzolá, F., Travaglini Allocatelli, C., Brancaccio, A., & Brunori, M. (1993) *FEBS Lett. 320*, 13−16.
Rohlfs, R. J., Mathews, A. J., Carver, T. E., Olson, J. S., Springer, B. A., Egeberg, K. D., & Sligar, S. G. (1990) *J. Biol. Chem. 265*, 3168−3176.
Smerdon, S. J., Dodson, G. G., Wilkinson, A. J., Gibson, Q. H., Blackmore, R. S., Carver, T. E., & Olson, J. S. (1991) *Biochemistry 30*, 6252−6260.
Smerdon, S. J., Krzywda, S., Wilkinson, A. J., Brantley, R. E., Carver, T. E., Hargrove, M. S., & Olson, J. S. (1993) *Biochemistry 32*, 5132−5138.
Springer, B. A., Egeberg, K. D., Sligar, S. G., Rohlfs, R. J., Mathews, A. J., & Olson, J. S. (1989) *J. Biol. Chem. 264*, 3057−3060.
Springer, B. A., Sligar, S. G., Olson, J. S., & Phillips, G. N., Jr. (1994) *Chem. Rev. 94*, 699−714.
Travaglini Allocatelli, C., Cutruzzolá, F., Brancaccio, A., Brunori, M., Qin, J., & La Mar, G. N. (1993) *Biochemistry 32*, 6041−6049.
Wittenberg, B. A., Brunori, M., Antonini, E., Wittenberg, J. B., & Wyman, J. (1965) *Arch. Biochem. Biophys. 111*, 576−579.
Wittenberg, J. B., Appleby, C. A., & Wittenberg, B. A. (1972) *J. Biol. Chem. 247*, 527−531.
Yamamoto, Y., Iwafune, K., Chûjô, R., Inoue, Y., Imai, K., & Suzuki, T. (1992) *J. Mol. Biol. 228*, 343−346.

BI9501592